UNIVERSITAT POLITÈCNICA DE CATALUNYA BARCELONATECH

Swansea University Prifysgol Abertawe

CENTRALE NANTES

Universität Stuttgart

MSc in Computational Mechanics

Computational Structural Mechanics and Dynamics

Practice 1: Plane Stress and Plane Strain

Submitted By:
Mario Alberto Méndez Soto
Eugenio Muttio Zavala
Daniel Thomas Benjaminsson

Submitted To:
Prof. Narges Dialami

Spring Semester, 2019

Exercise 1 - Thin plate under dead weight

A thin plate, as shown in Figure (1), subject to its self-weight and it is constrained on its upper face to the support. A convergence analysis and study of the accuracy of the mesh will be carried out using triangular elements with 3 and 6 nodes and quadrilaterals with 4, 8 and 9 nodes. The exact solution is given to be:

- Displacement of the center of side ED u_y equals $2.26E-6$ mm
- Stress σ_y at point B equals $0.247MN/m^3$

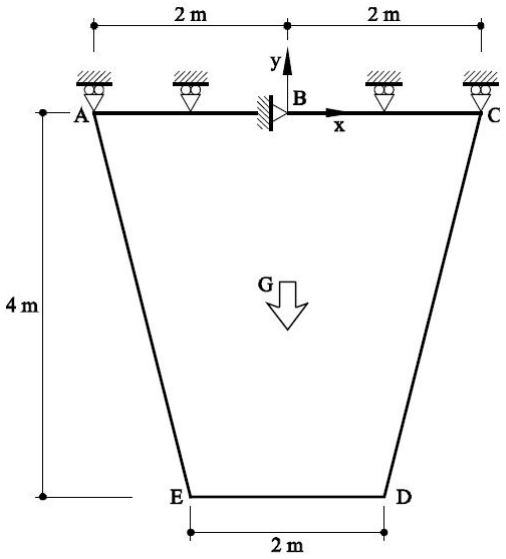

Fig. 1 – Thin plate - geometry and boundary conditions

The plate is made of a material with the following physical properties.

- Young Modulus $E = 2.1E5MPa$
- Poisson coefficient $\nu = 0.30$
- Specific Weight $\gamma = 7000\frac{kg}{m^3}$
- Thickness $t = 0.1m$

Discretized models with triangular and quadrilateral elements are shown in Figure (2). Please note that the meshes depicted correspond to the finest meshes used in the convergence study.

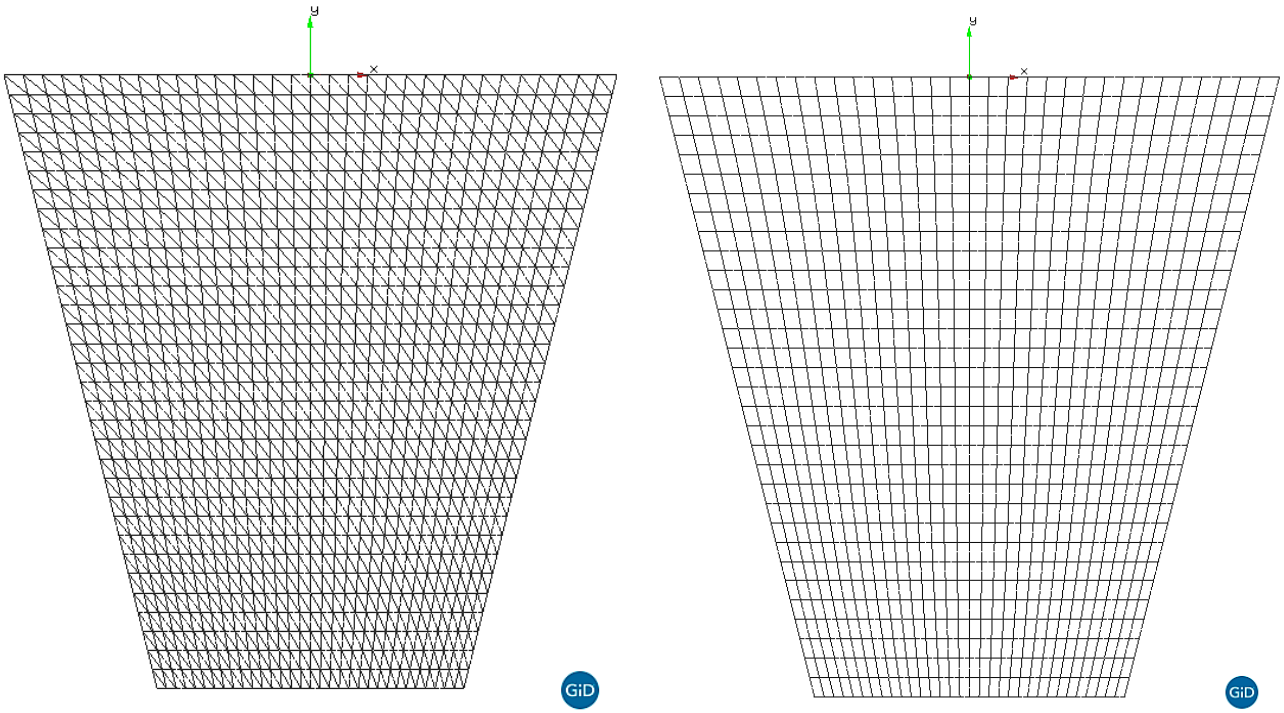

(a) (b)

Fig. 2 – Mesh using triangular (a) and quadrilateral (b) elements

Results for the vertical displacements and corresponding stresses using linear triangular elements are shown in Figures (3) and (4).

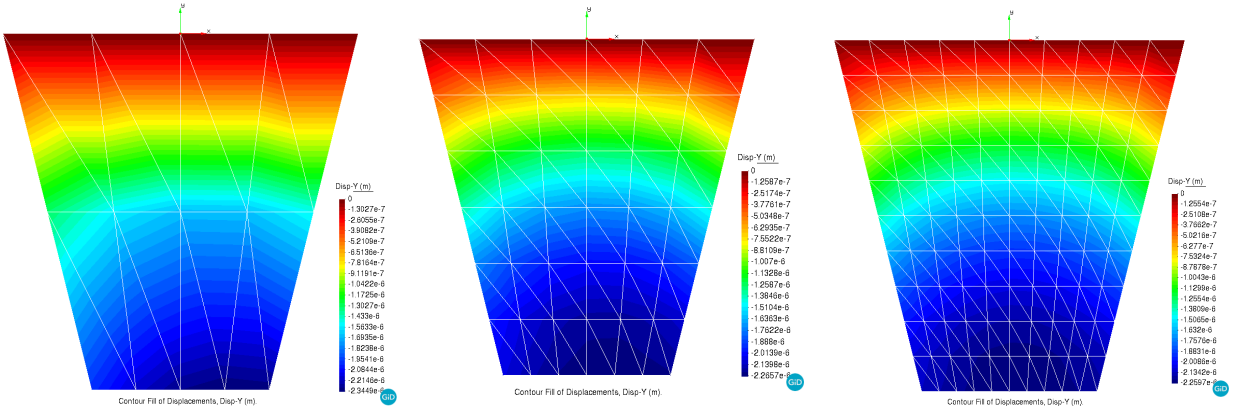

(a) (b) (c)

Fig. 3 – Vertical displacement results using 16 (a), 72 (b) and 200 (c) triangular linear elements

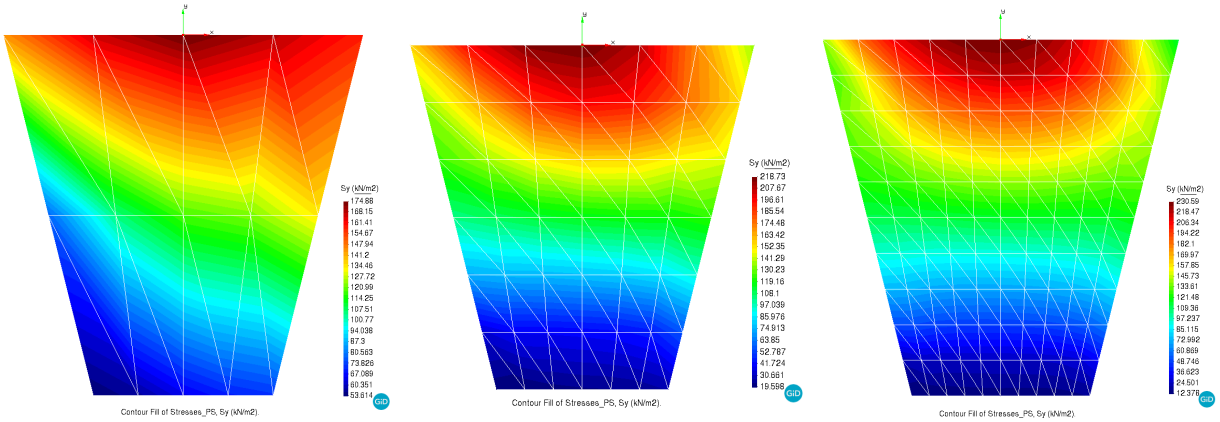

(a) (b) (c)

Fig. 4 – Stress fields σ_y results using 16 (a), 72 (b) and 200 (c) triangular linear elements

Results for the vertical displacements and corresponding stresses using linear quadrilateral elements are shown in Figures (5) and (6).

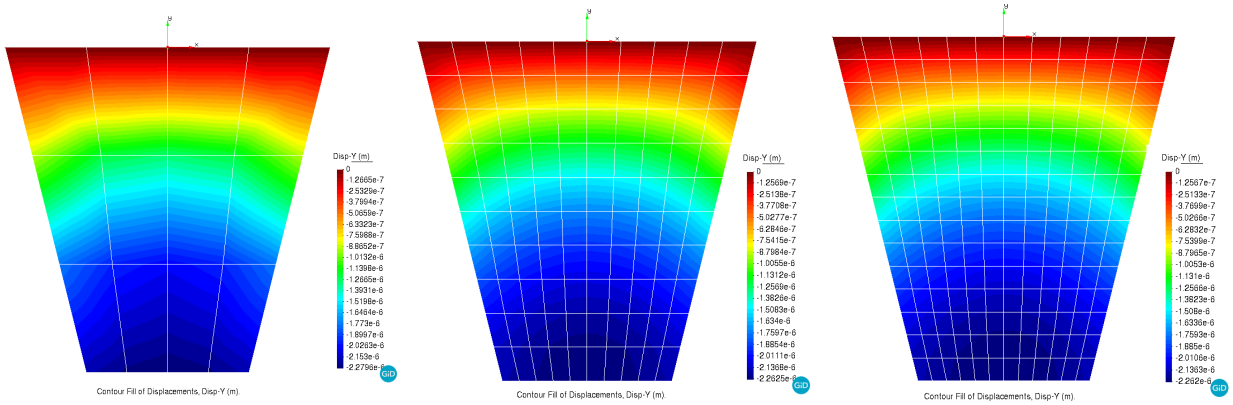

(a) (b) (c)

Fig. 5 – Vertical displacement results using 12 (a), 100 (b) and 180 (c) quadrilateral linear elements

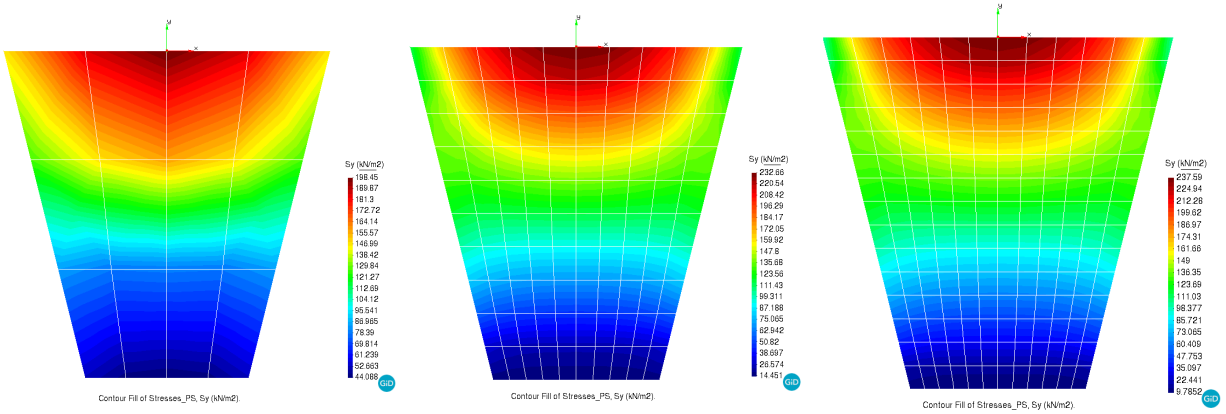

Fig. 6 – Stress fields σ_y results using 12 (a), 100 (b) and 180 (c) quadrilateral linear elements

The following figures present a diagram of the convergence rate of each of the analyzed elements:

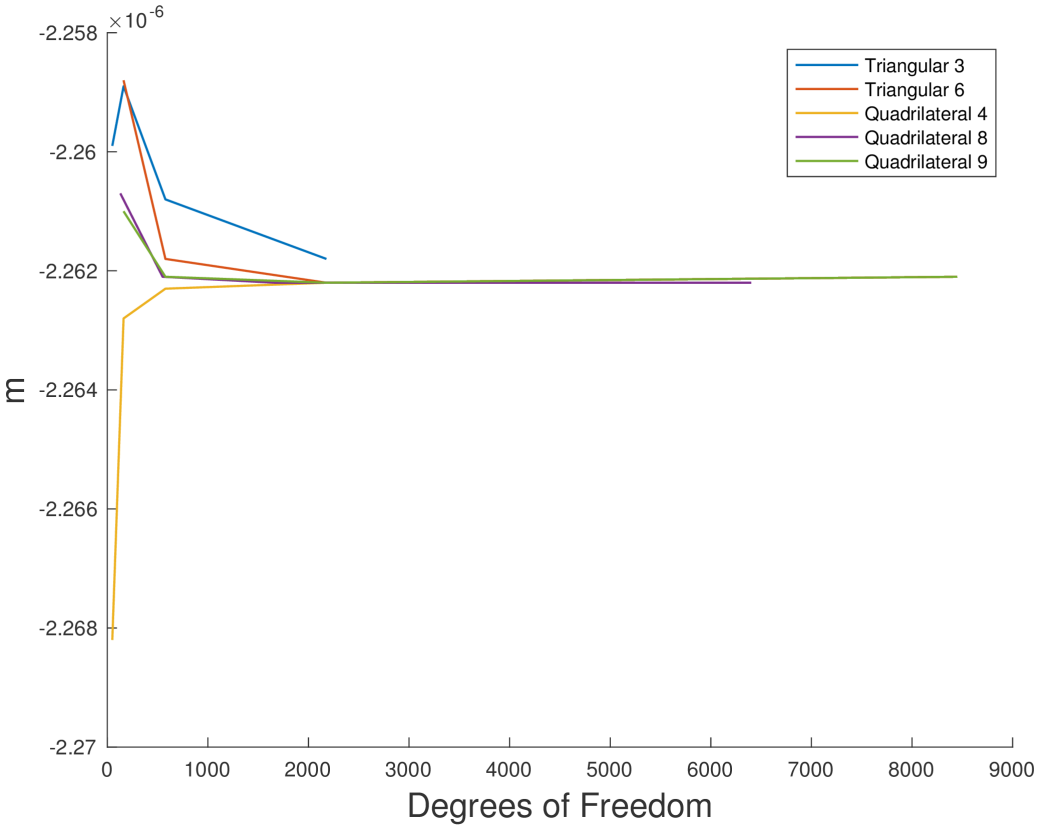

Fig. 7 – Convergence of the value of the displacement of the center of side ED u_y

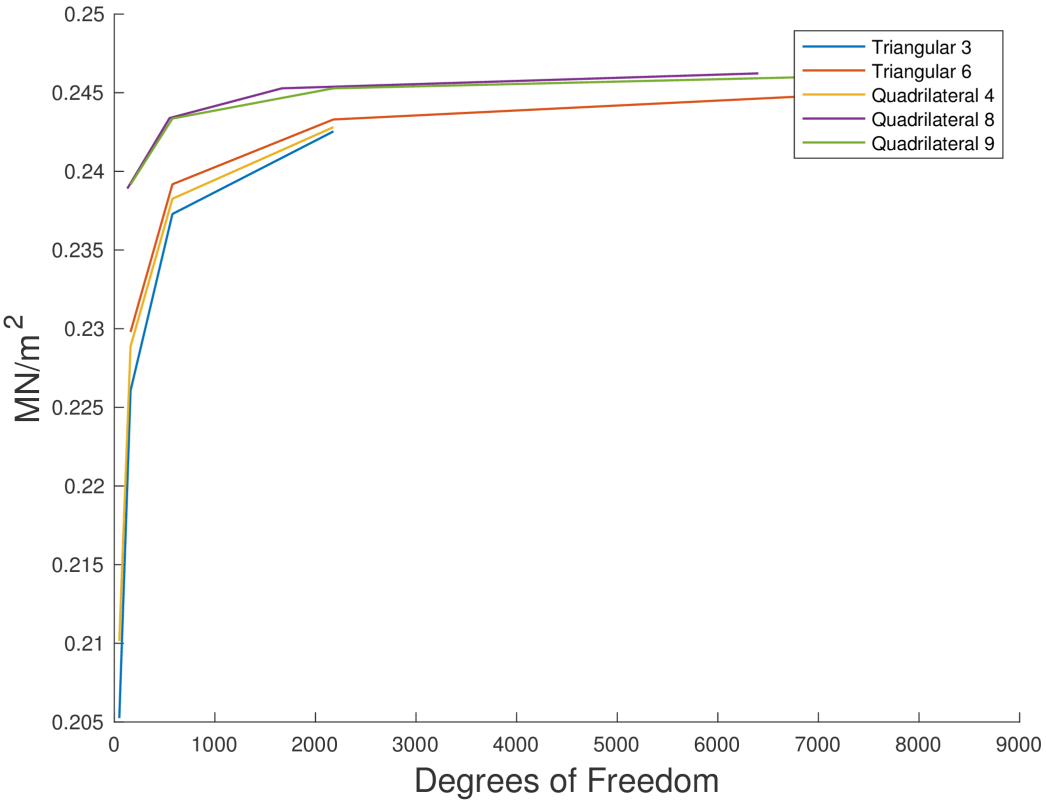

Fig. 8 – Convergence of the value of the stress σ_y at point B

Exercise 2 - Plate with two sections

The structure in Figure (9) presents a reinforced concrete plate with two holes, supported by three columns. The central column undergoes a displacement δ due to sag of the foundation caused by a leakage in some pipes nearby. The geometry of the structure and the loads applied are shown in Figure 9. The material properties used in the analysis can be found below.

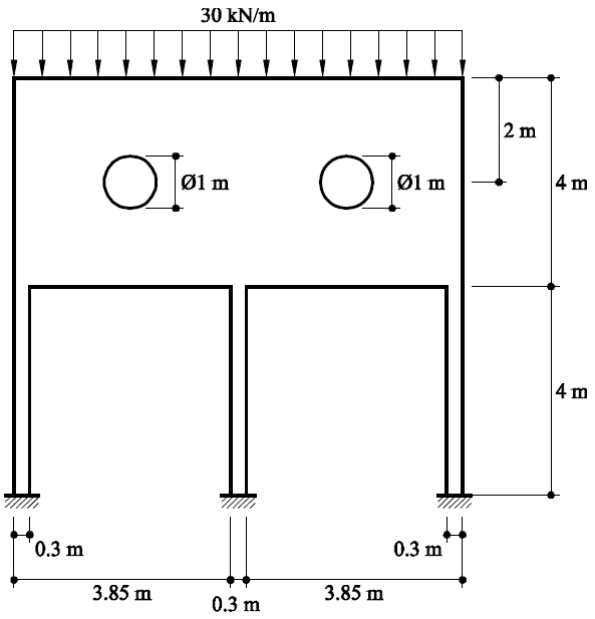

Fig. 9 – Reinforced concrete plate with two holes: geometry and loads applied.

- Young Modulus $E = 3.0E10\frac{N}{m^2}$
- Poisson coefficient $\nu = 0.2$
- Specific Weight $\gamma = 24000\frac{N}{m^3}$
- Thickness $t = 0.2m$

In order to analyze the effect of a displacement of 1 cm on the stability of the structure, a FEM stress analysis with linear triangular elements (see Figure 10) is carried out. As it can be seen, the mesh is refined in the zones where the gradients of stresses are expected to be greater, which are in the connection of the column with the plate. Firstly, the solution is found for no imposed displacements on the central column.

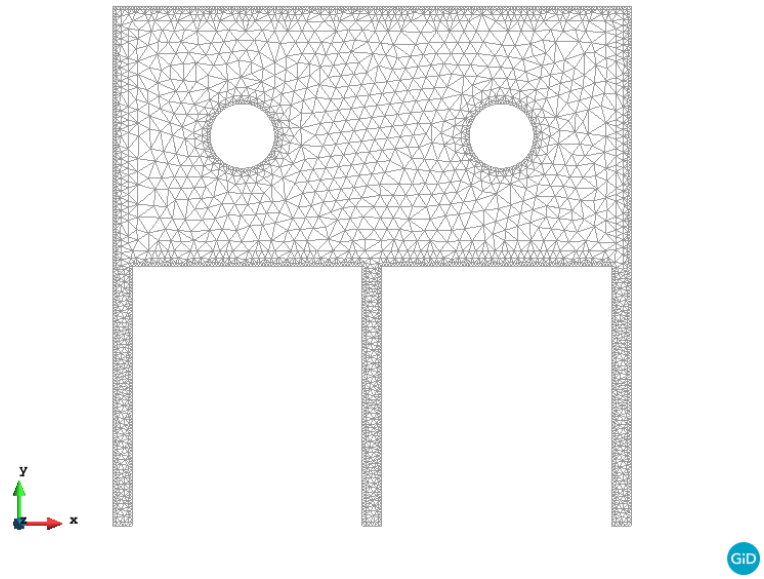

Fig. 10 – Discretization of the problem with 3,389 nodes (5694 elements)

As a first result, it is worth depicting the deformed state of both models, whence the imposed displacement on the central column is clearly visible, and its effect on the rest of the structure is noticeable (see Figure 11).

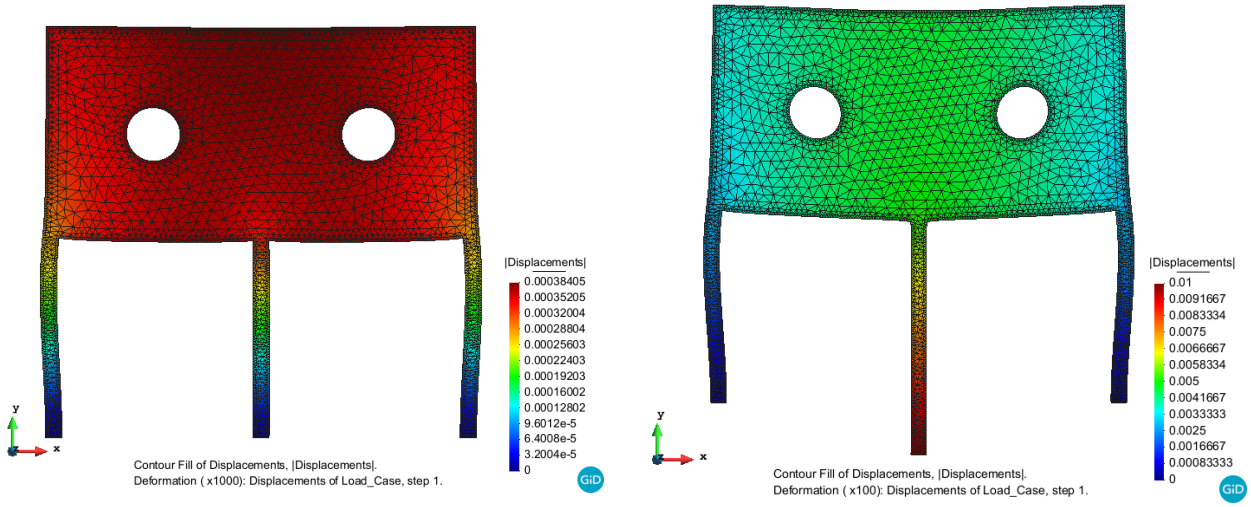

(a) (b)

Fig. 11 – Deformed state of the (a) original structure and (b) structure with imposed displacement.

The stress state analysis results are shown in Figures (12), (13), (14) and (15). A discussion of the stress results is presented next:

- **Stress** σ_x : The results exhibit that the original model (Fig 12a) presents a regular behavior

with tension stress on the lower layers of the plate and some compression on the upper ones. In contrast with Figure (12b), in which both values of stress increments are almost 30 times approximately, and in the connection of between the central column and the plate, the value of tension changes from 854 KN/m^2 $[C]$ to 24906 KN/m^2 $[T]$.

- **Stress** σ_y : A comparisong of Figures (13a) and (13b), allows to notice the change in the behavior due to the sag of the foundation. The central column working originally in compression, now is completely tensed and the maximum tensile values of stresses increased from 93 KN/m^2 $[T]$ in the plate to 42964 KN/m^2 $[T]$ in the central column. The compression is incremented ten times and then distributed completely between the two side columns.

- **Stress** τ_{xy} : Considering Figures (14a) and (14b), it is shown again that there is a considerable increase in the stresses, and also it is worth mentioning that the two holes in the plate could cause critical problems since the increment is affecting this part of the structure as well.

- **Principal Stresses:** The results showed an important change due to the change in behavior of the complete structure by imposing a displacement of only 1 cm in the central support. As seen in Figure (15a), first the columns work in compression as a regular frame, but then in figure (15b) the central column is completely tensed. Moreover, the direction of the stress vector vary significantly including now tension vectors.

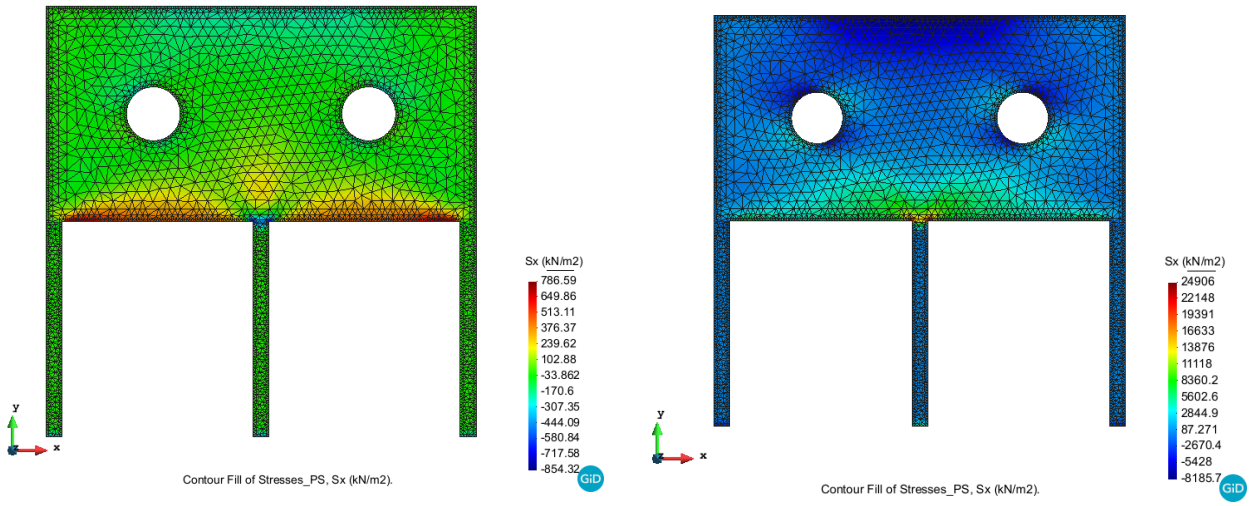

(a) (b)

Fig. 12 – Stress σ_x of the (a) original structure and (b) structure with imposed displacement.

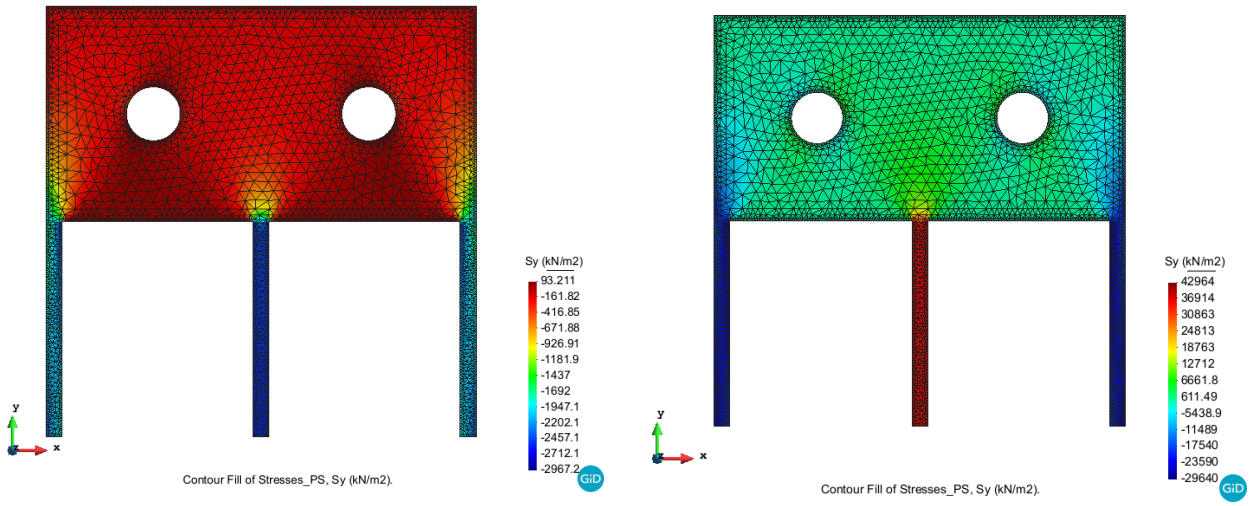

(a) (b)

Fig. 13 – Stress σ_y of the (a) original structure and (b) structure with imposed displacement.

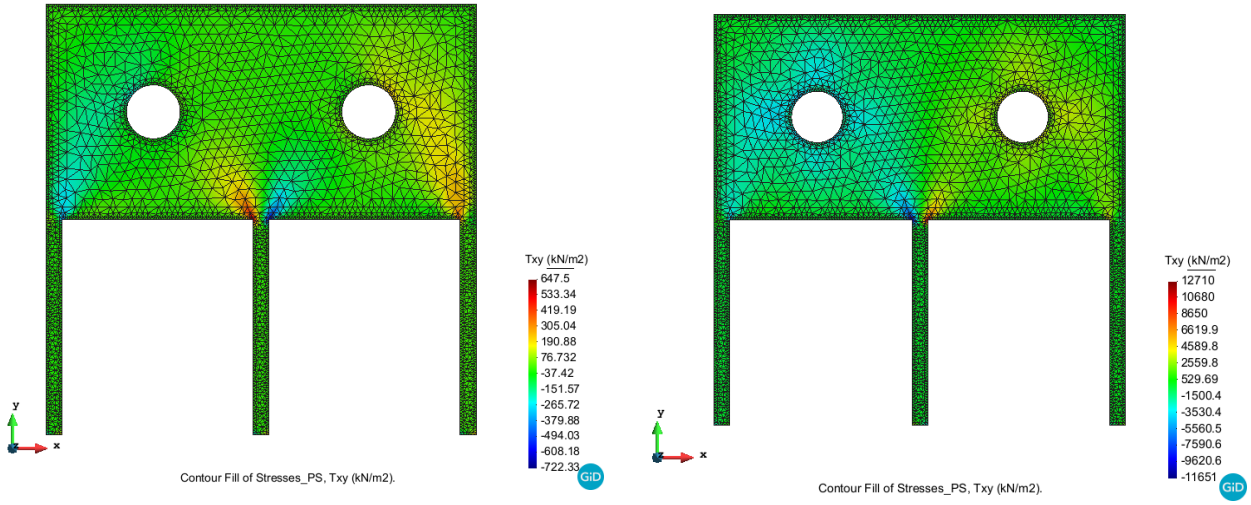

(a) (b)

Fig. 14 – Stress τ_{xy} of the (a) original structure and (b) structure with imposed displacement.

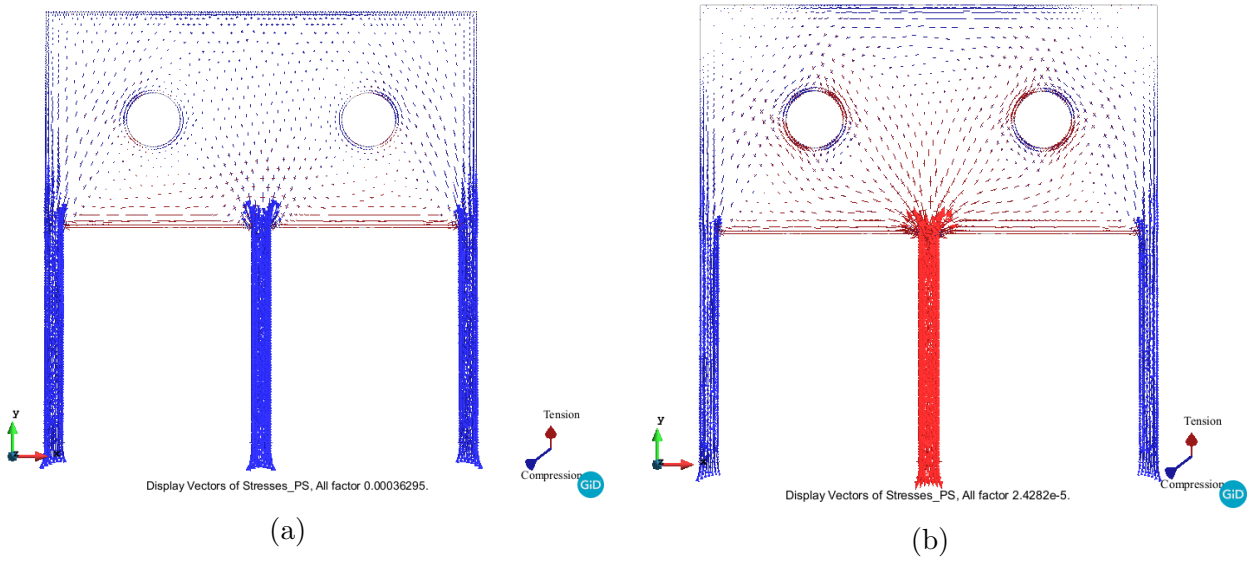

(a) (b)

Fig. 15 – Principal stresses of the (a) original structure and (b) structure with imposed displacement.

Exercise 3 - Plate with ventilation hole

The structure represents a reinforced concrete plate with simple supports. This plate possesses a hole for a ventilation pipe. Due to a change in the initial project, the design load for which the plate was calculated increased significantly. This motivated the placement of a metal reinforcement sheet on both sides of the plate in the area of the hole. The geometry, loads and constraints are depicted in Figure (16).

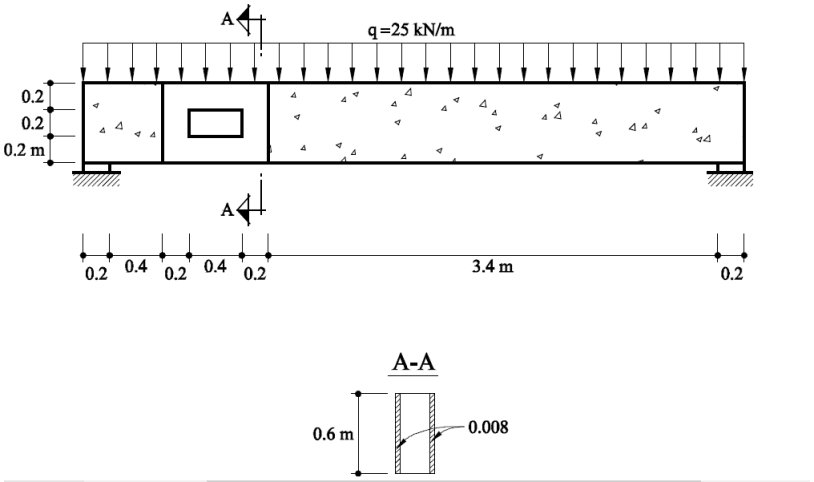

Fig. 16 – Plate with ventilation hole geometry, loads and constrains project.

In order to verify if the reinforcement proposal is suitable and actually necessary, a FEM analysis will be performed considering both the original full-concrete structure and a second one with steel plates confining the ventilation hole (as showed in the cross section A-A in Figure (16)). The material properties considered are the following ones:

- **Concrete**
  - Young Modulus $E = 3.0E10\frac{N}{m^2}$
  - Poisson coefficient $\nu = 0.2$
  - Specific Weight $\gamma = 24000\frac{N}{m^3}$
  - Thickness $t = 0.25m$
- **Steel**
  - Young Modulus $E = 2.1E11\frac{N}{m^2}$
  - Poisson coefficient $\nu = 0.3$
  - Specific Weight $\gamma = 78000\frac{N}{m^3}$
  - Thickness $t = 0.016m$ (2 plates)

For the FEM analysis, the domain is discretized with 2,450 linear quadrilateral elements (see Figure (17)) with refinements around the vicinity of the ventilation hole. As for the second model, overlapping meshes (with collapsed nodes) for both the steel and concrete structures were used, assuring thus compatibility of the displacements.

The computations of the deformed state (see Figures (18a) and (18b)) revealed that the displacements of the reinforced beam are slightly greater in comparison (around $0.02mm$), which can be explained considering the weight of the steel plates.

Since the ventilation hole will be the place of a pipe, it is vital to take into account the deformation in the region around the hole itself, to check for not admissible too large strains. Thus,

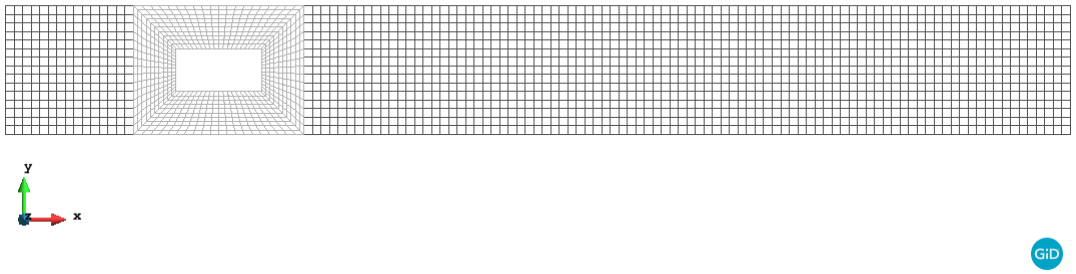

Fig. 17 – Discretization of the problem. Two colors are shown to indicate the materials.

once again the results showed that the difference between the original and reinforced models are practically negligible, i.e. the deformation state is not a critical factor to considering.

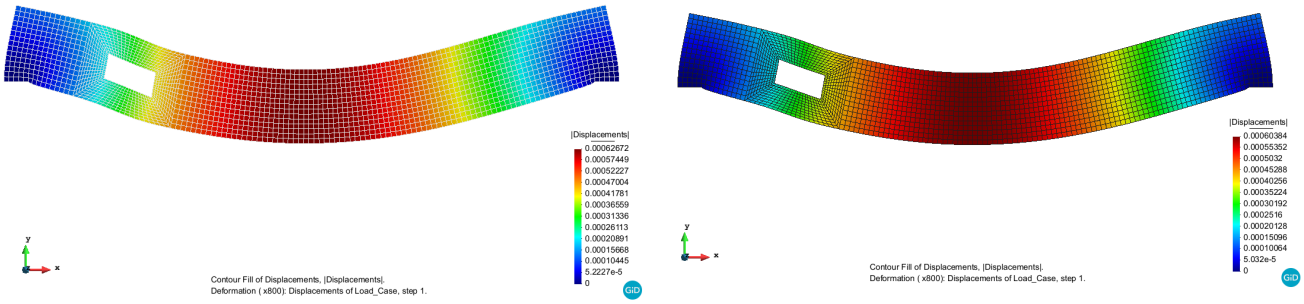

(a) (b)

Fig. 18 – Deformed state of the (a) concrete (b) concrete-steel models

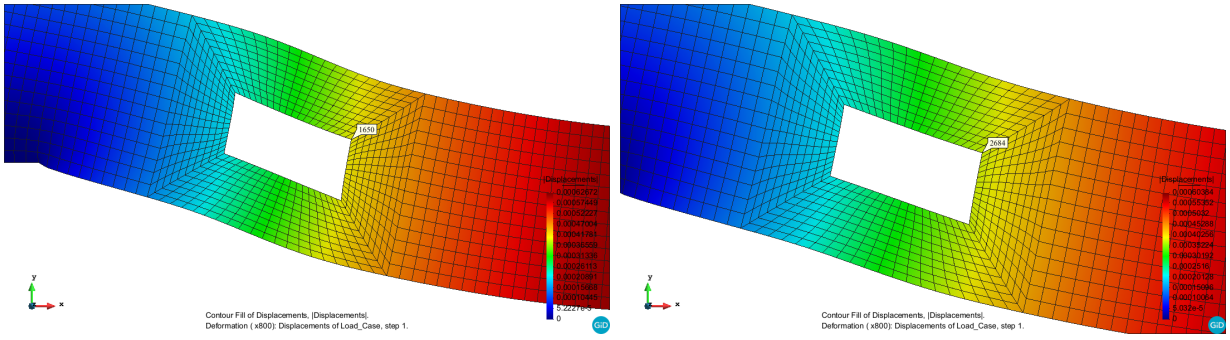

(a) Concrete model deformation of node is equal to 0.4076 mm

(b) Concrete-steel model deformation of node is equal to 0.37828 mm

Fig. 19 – Deformation of a point in the vicinity of the hole for (a) concrete (b) concrete-steel models

The second part of the analysis is to verify the stress state of the original concrete model and the reinforced one. As the representations of the stresses vector fields show in σ_x direction (see Figure 20), there is a general detriment of around 0.02% in the critical stresses of the plate (even for σ_y and τ_{xy}, which are not relevant to include). For instance, in the mid-point of the model, where tension (lower nodes) and compression (upper nodes) are involved, as well as the reactions. The general reduction observed when using the reinforcement is beneficial, but does not affect considerably the behavior of the entire system. Once again, it becomes more important to check the state stress of nodes in the vicinity of the hole (consider results shown in Figures (21), (22), and (23)).

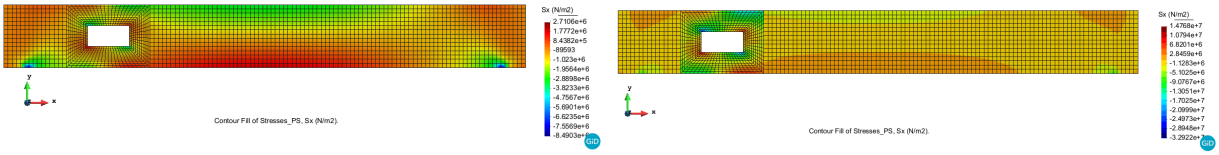

(a) (b)

Fig. 20 – σ_x stress in (a) concrete (b) concrete-steel models

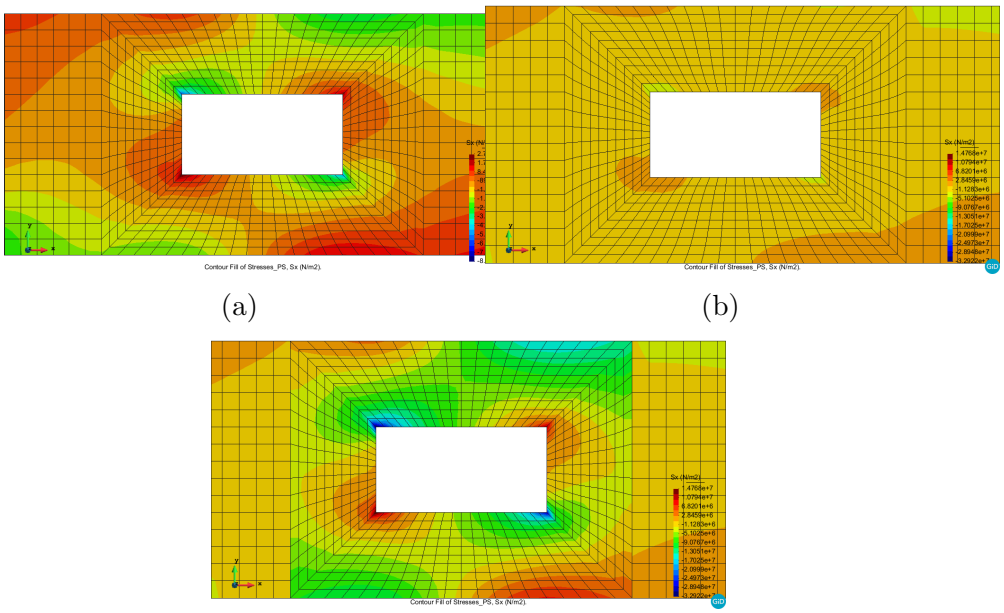

(a) (b)

(c)

Fig. 21 – Stress σ_x in the region of the ventilation hole in the (a) concrete (b) reinforced concrete (c) steel plate models

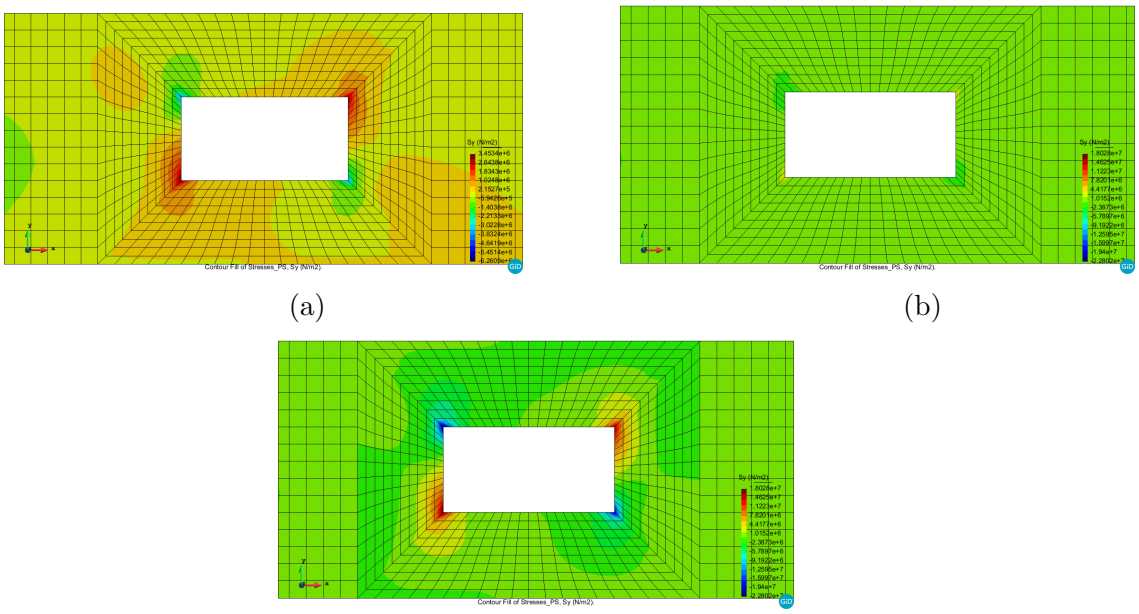

(a) (b)

(c)

Fig. 22 – Stress σ_y in the region of the ventilation hole in the (a) concrete (b) reinforced concrete (c) steel plate models

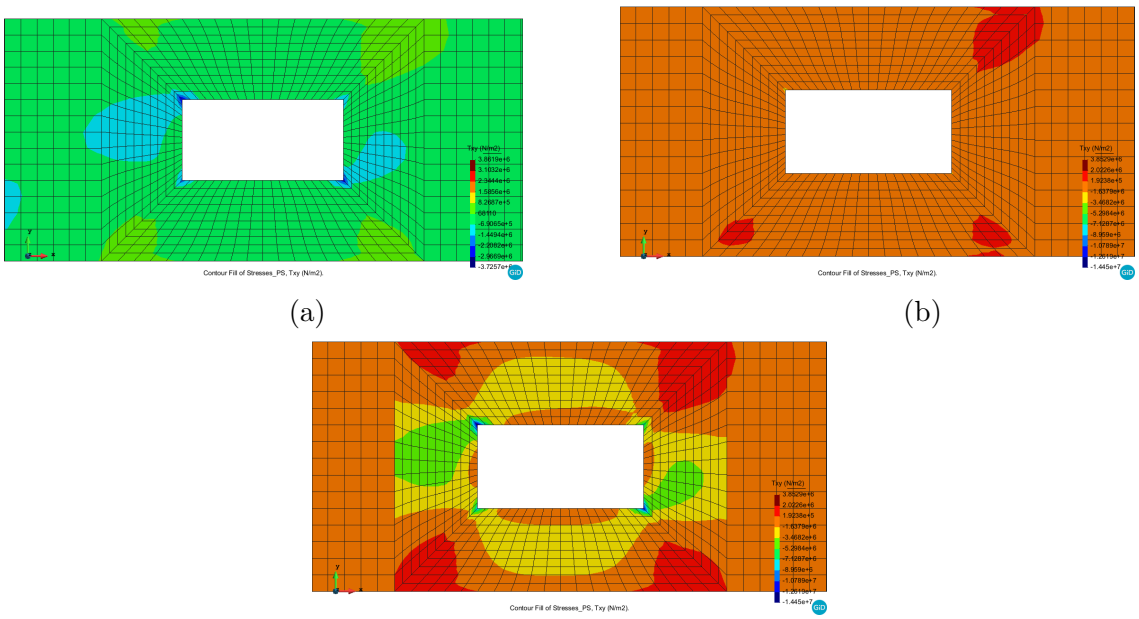

(a) (b)

(c)

Fig. 23 – Stress τ_{xy} in the region of the ventilation hole in the (a) concrete (b) reinforced concrete (c) steel plate models

The previously presented results of stress states in the region of the ventilation hole allow us to make a final decision on whether to include or not the steel reinforcement. As it can be seen, at the corners of the hole an important reduction (around 25%) in the tension stress values is exhibited, which are one of the mandatory critical values to review since the concrete by itself cannot sustain this type of loading as evident in the latter representations of the stress fields (σ_x, σ_y, τ_{xy}). A vector field representation of the principal stresses in the vicinity of the hole (see Figure (24)), allow us to better understand the difference between the two proposed solutions and to observe how the tension and compression affect the critical points in the model. Thus, as a conclusion, it is possible to state that whether the steel plate is required or not will depend on *the concrete reinforcement design of the beam*, because if the engineer in charge has considered in the design enough steel rebars to resist the tension stresses presented in the ventilation hole, then **the metal plate is not needed**. Otherwise, if the steel rebars are optimal for just the concrete, and the tension presented in this analysis is greater than the ones from the rebars, then **the metal plate is needed**

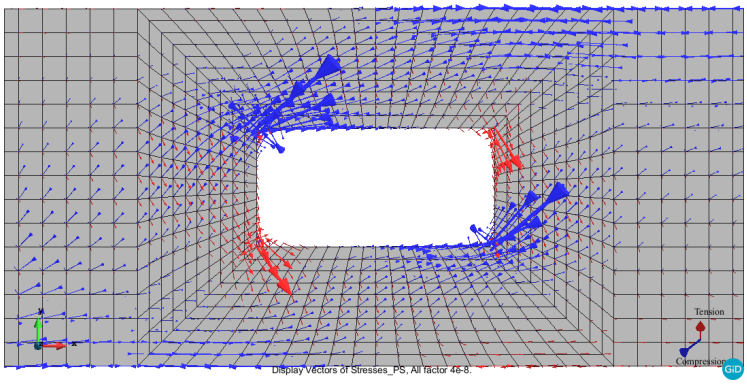

(a)

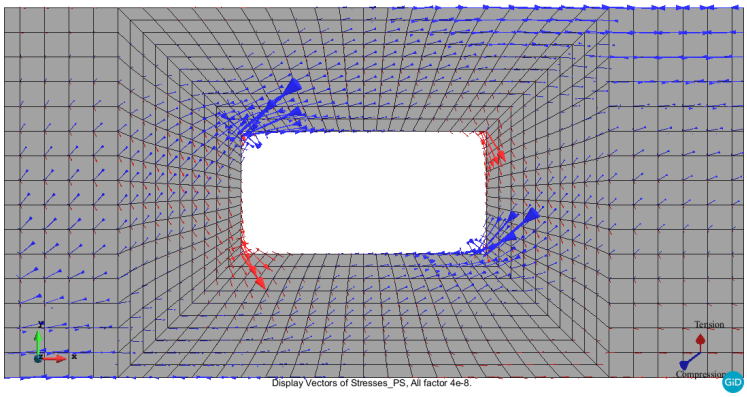

(b)

Fig. 24 – Principal stresses in the vicinity of the ventilation hole for the (a) concrete model (b) concrete-steel models

Exercise 4 - Prismatic water tank

A 3-meter-high rectangular tank is used to store drinking water. The cross section of the tank and its geometric dimensions are depicted in Figure (25).

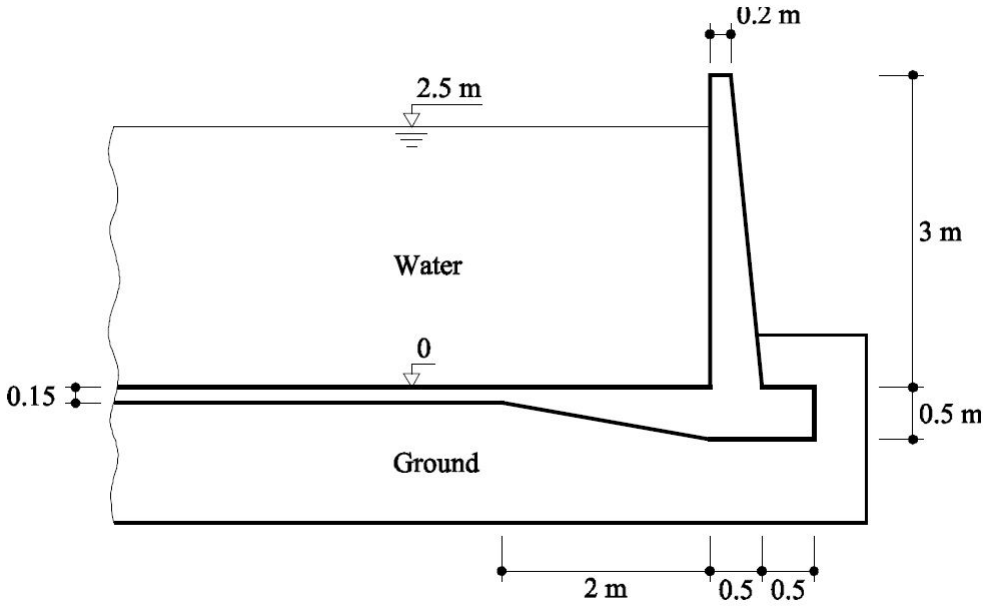

Fig. 25 – Cross section of the water tank

For the analysis of the problem, the domain was discretized using a unstructured mesh with 1,059 quadrilateral elements (see Figure (26a)) with linear shape functions. A more in-depth analysis would eventually need mesh refinements in the vicinity of sharp corners.

The water column is modeled using two separate hydrostatic distributed loads at the bottom and vertical wall of the tank (maximum value at the bottom equal to $\rho h g_{H_2O} = 24500 N/m$), whereas, the ground is modeled as an elastic support with load coefficient equal to $50 N/cm^3$. The weight of the structure is also taken into account in the computations. Moreover, it is assumed that the ground can only resist compression efforts with no traction or resistance in the x direction allowed. A symmetry condition was imposed on the left boundary of the model, restricting the displacements on the x direction (see Figure (26b)).

The problem is considered to be a plane strain problem with concrete as the material of the water tank structure ($E = 30.0e10 N/m^2$, $\nu = 0.2$, $\gamma = 24000 N/m^3$).

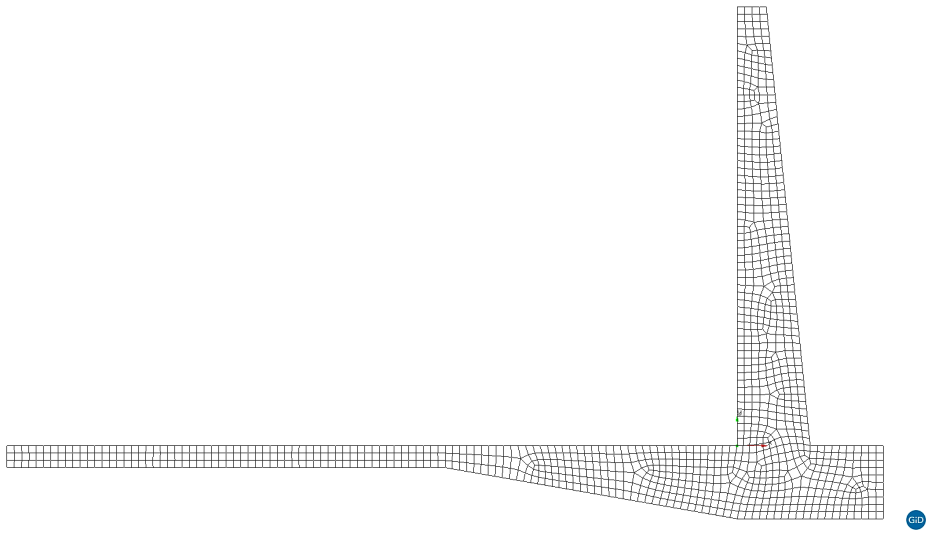

(a)

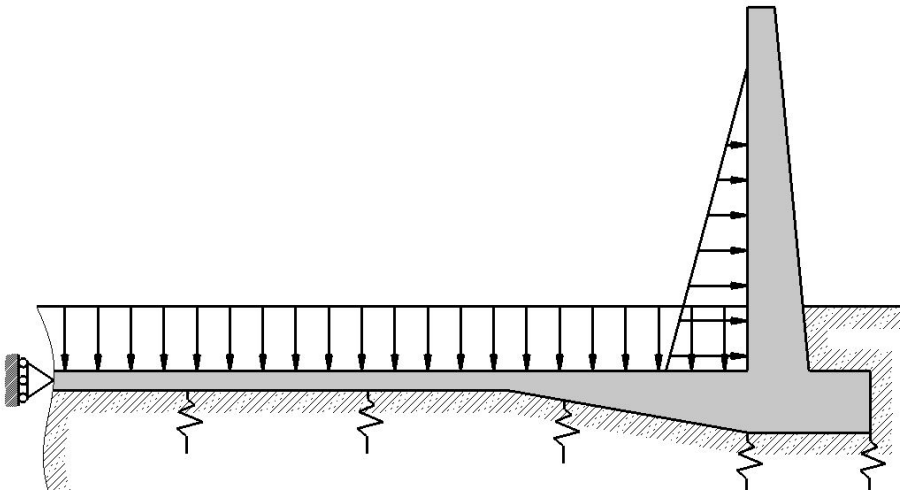

(b)

Fig. 26 – Discretized model (a) and boundary conditions (b) of the computational model

An analysis of the stress vectors allows us to verify the correctness of the problem. As stated before, the ground cannot sustain tension efforts which is satisfied based on the results depicted in Figure (27). Only compression stresses are obtained at the boundary of the ground matching thus the physics of the problem.

The displacements (m) and the corresponding deformed configuration (with a factor of 250) are depicted in Figure (28). The displacements reach their maximum value at the top of the structure (around 1 m) and as expected the displacements are more pronounced in the x direction and less important in the y direction due to the elastic compensating effect of the ground.

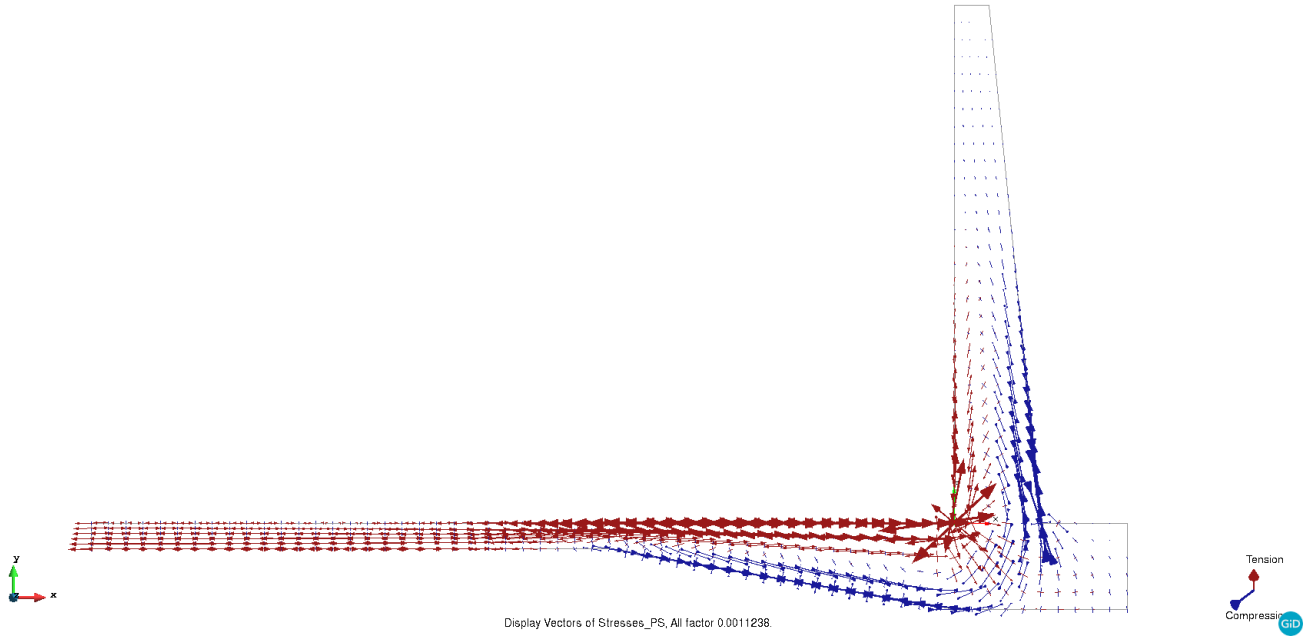

Fig. 27 – Stress vector field

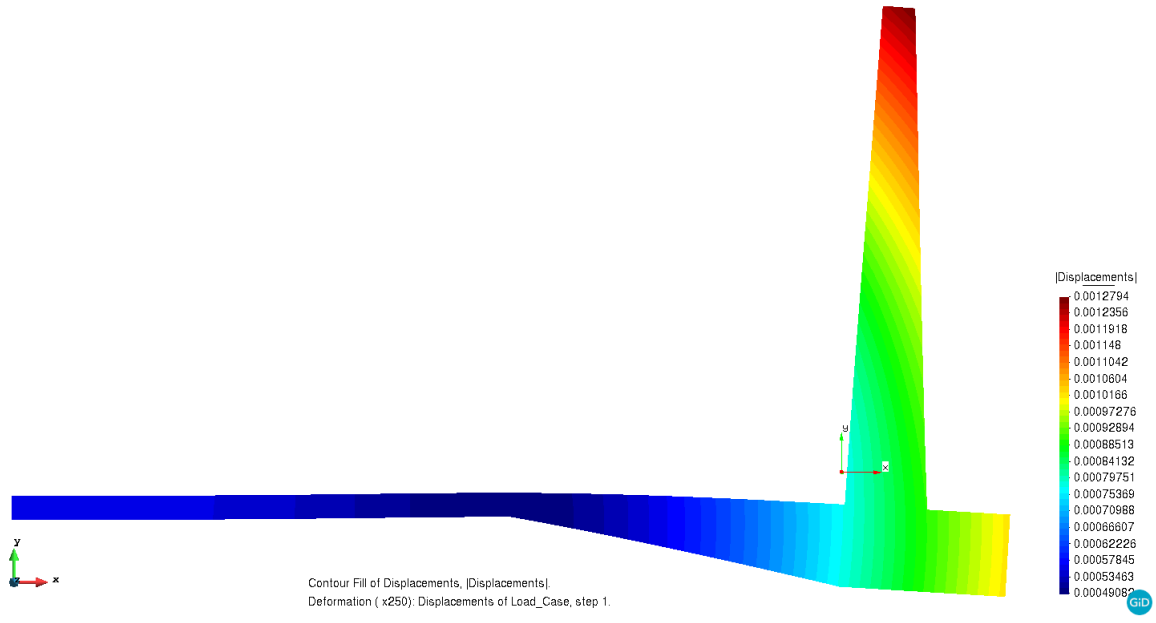

Fig. 28 – Displacement results

The normal stresses in the x, y and z are represented in Figure (29). The maximum normal stress values reached are $607kN/m^2$, $470kN/m^2$ and $177kN/m^2$ for the x, y and z directions, respectively. The maximum x stress is computed to be at the bottom of the tank due to the normal pressure of the water causing the bottom of the tank to be "pulled" whereas the area in contact with the ground is compressed. Similarly, the deformation of the structure is such that the vertical wall of the tank is bent in the x direction, causing the internal face to be subject to tensile stresses while the external face is under compression. Hence, the results of the simulation showed that the greatest value of stresses will be in the vicinity of the connection between the bottom and the vertical wall of the structure, where additional care should be taken in order to assure the structure can withhold the given loading conditions.

In order to obtained more reliable results mesh refinements would be needed in the region of sharp corners subject to the maximum stresses. Furthermore, if the displacements or the stresses surpass the permissible values, reinforcements can be considered in the form of steel internal bars and other possible engineering composite solutions.

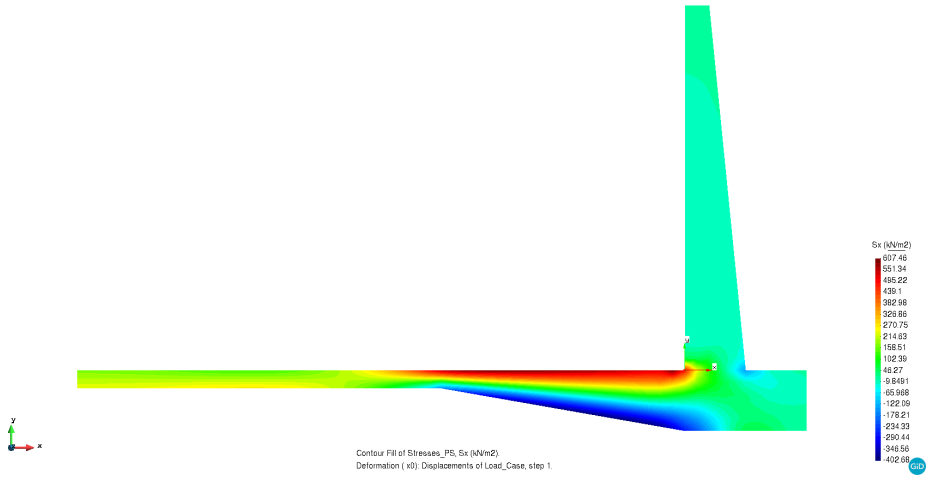

(a) Normal stresses in the x-direction

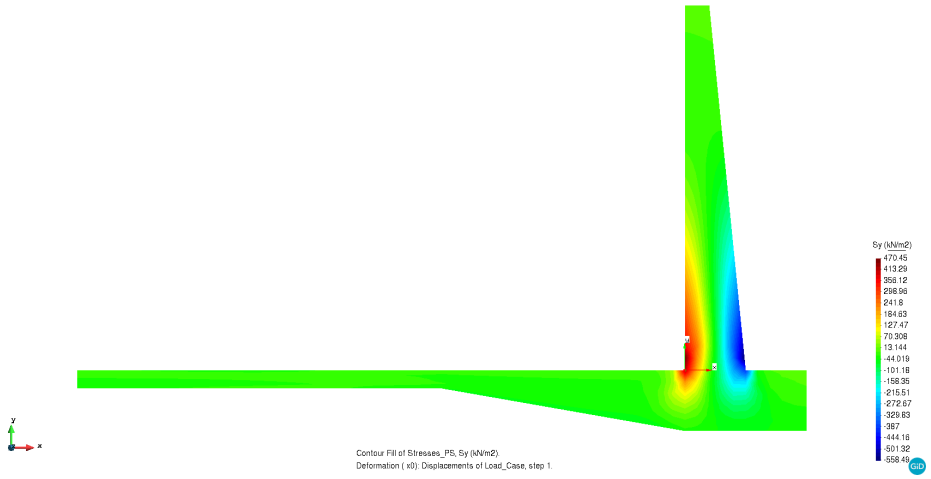

(b) Normal stresses in the y-direction

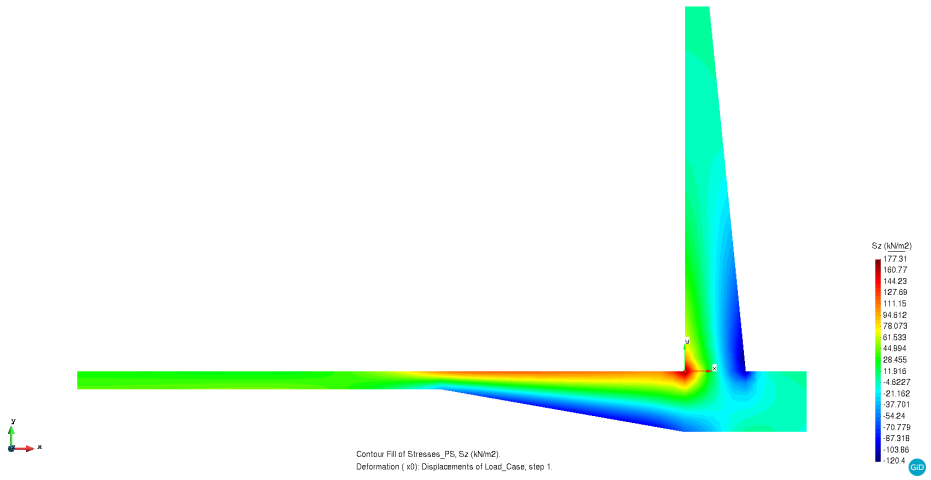

(c) Normal stresses in the z-direction

Fig. 29 – Normal stress vector fields